Polymer 51 (2010) 475–481

Contents lists available at ScienceDirect

Polymer

journal homepage: www.elsevier.com/locate/polymer

Polymer conformation-assisted wrapping of single-walled carbon nanotube: The impact of *cis*-vinylene linkage

Wenhui Yi [a,1], Andrey Malkovskiy [b], Yongqian Xu [a], Xiao-Qian Wang [c], Alexei P. Sokolov [b], Marisabel Lebron-Colon [d], Michael A. Meador [d], Yi Pang [a,*]

[a] Department of Chemistry, University of Akron, OH 44325, USA
[b] Department of Polymer Science, University of Akron, OH 44325, USA
[c] Department of Physics and Center for Functional, Nanoscale Materials, Clark Atlanta University, Atlanta, GA 30314, USA
[d] Structures and Materials Division, NASA Glenn Research Center, Cleveland, OH 44135, USA

ARTICLE INFO

Article history:
Received 22 September 2009
Received in revised form
30 October 2009
Accepted 13 November 2009
Available online 4 December 2009

Keywords:
Carbon nanotube
Conjugated polymer
Fluorescence

ABSTRACT

A soluble π-conjugated polymer *cis*-P*m*PV is found to be twice as effective as its *trans*-P*m*PV isomer in dispersing SWNTs into organic solvents. The improved efficiency is related to the specific conformation of *cis*-vinylene-enriched P*m*PV, which facilitates a planar π–π interaction with SWNT surface and leads to improved nanotube dispersion. ^{1}H NMR spectra indicate that the *cis*-CH=CH bonds are partially converted to the *trans*-CH=CH, thereby providing necessary conformational cavity for SWNT wrapping. Irradiation triggers a precipitation from SWNT dispersion, providing a purified SWNT/conjugated polymer composite.

1. Introduction

Single-walled carbon nanotubes (SWNTs) are rolled graphite sheets along a certain angle or vector. The electronic structure and optical properties of individual SWNT are dependent on the specific rolling angle between the graphene lattice and the nanotube axis, which defines the chiral indices (n, m) and separates the tubes into metallic and semi-conducting forms [1]. The combination of superior electronic and mechanical properties of SWNTs has led to their use in various applications, including flexible electronics [2], biosensors [3], and transistors [4]. In the as-prepared sample, the individual tube is strongly held together with others within a mixture of metallic and semi-conducting tubes. The notorious insolubility of the bundled SWNTs limits their full utilization in materials and devices. Realization of the true potential of SWNTs in those applications listed above, therefore, is dependent on our fundamental understanding, not only of how to effectively disperse the bundled SWNTs but also of how to isolate a specific SWNT from the mixture of the various tubes.

An effective strategy to solubilize SWNTs relies on ultrasonication-enforced segregation of nanotube species out of entangled bundles in the presence of a non-reactive dispersing reagent. A strong interaction between the added reagent and a SWNT is necessary to disperse a tightly held SWNT from the bundle. The maximum interaction will take into consideration the electronic properties, chiralities and diameters (or size) of the existing SWNTs in the mixture. A wide-range of surfactants, small molecules, and polymers have been utilized for this purpose and have been reviewed in a recent article [5]. Among these dispersing agents, π-conjugated polymers are of special interest, since their backbones can form a uniquely ordered three-dimensional structures that lead to well-defined SWNT–polymer interactions. It should be noted that every polymer has its own tendency to form a specific conformation, which can be tailored to enhance the polymer's interaction with SWNTs. Utilization of this conformational effect, which a small molecular surfactant cannot match, has the potential to achieve the optimum polymer/SWNT interaction, thereby improving the nanotube dispersion efficiency.

Poly[(*m*-phenylenevinylene)-*alt*-(*p*-phenylenevinylene)] (P*m*PV) derivatives **1** have been extensively investigated for use as a polymeric dispersion agent for SWNTs [6,7,8,9]. The *meta*-phenylene linkages in **1** provide the bent angles along the polymer backbone, which are necessary to form a helical conformation. The intrinsic ability of P*m*PV to form a helical conformation is thought to be

* Corresponding author.
E-mail address: yp5@uakron.edu (Y. Pang).
[1] Present address: Department of Electronic Science and Technology, Xi'an Jiaotong Univeristy, China.

0032-3861/$ – see front matter © 2009 Elsevier Ltd. All rights reserved.
doi:10.1016/j.polymer.2009.11.052

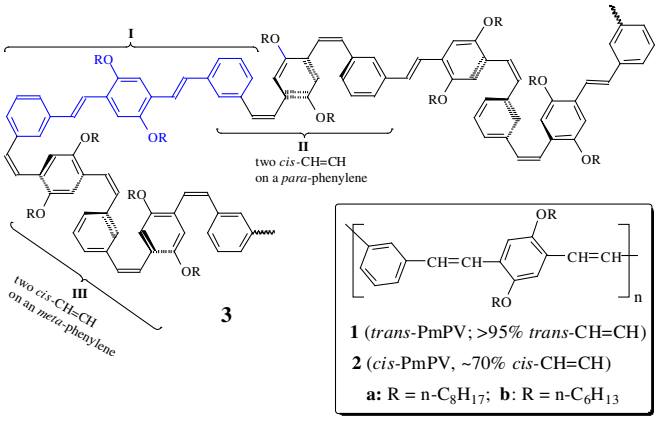

Scheme 1. The chemical structure of *trans*-P*m*PV **1** and *cis*-P*m*PV **2** (insert at the right bottom). And the possible chain structure of *cis*-P*m*PV in THF (**3**).

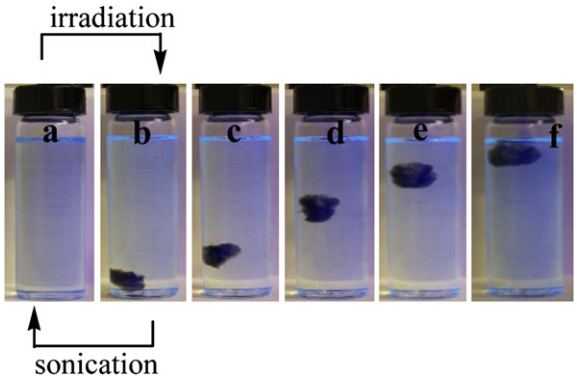

Fig. 1. Images of *cis*-P*m*PV and SWNTs in THF: (a) as-prepared suspension; (b) precipitation after irradiation with 300–500 nm for 1 h. The images b, c, d, e, and f show that the entire precipitated mass was floating up together under irradiation with a portable UV-lamp (365 nm).

responsible for its good tube dispersion capability, with **1a** ($R = n$-C_8H_{17}, Scheme 1) showing a preference for SWNTs of 1.35–1.55 nm [10,11] and **1b** ($R = n$-C_6H_{13}) for SWNTs of 1.1–1.3 nm diameters [12]. The impact of side chains on the tube size selectivity can be attributed to their ability to influence the polymer conformation. Application of the composite **1**/SWNTs includes electrical conducting films [13,14] and optoelectronic memory devices [15].

A π-conjugated polymer surfactant for SWNTs should exhibit good solubility, because the molecule has to exfoliate SWNT bundles and bring the individual tube into solution. The *cis*-vinylene-enriched **2** (Scheme 1), which is the geometrical isomer of **1** ($\alpha \approx 1.0$), is known to have superior solubility in organic solvents, attributing to its lower Mark–Houwink α exponent ($\alpha \approx 0.85$) [16]. Although good solubility suggests that polymer **2** could be an effective de-bundling agent, no successful example [17] has been reported to effectively de-bundle the nanotubes by using **2**. The poor dispersion of SWNTs by using **2a** is thought to be due to polymer's self-aggregation that inhibits its interaction with SWNTs [17,18]. A literature survey shows that little is known about the role of *cis*-CH=CH in the nanotube dispersion. Herein we report that polymer **2b** (*cis*-P*m*PV) is a superior dispersing reagent for SWNTs than its isomer **1b**. The study reveals the significant impact of *polymer conformation* and *cis-vinylene bond geometry* on the tube wrapping.

2. Results and discussion

A pure SWNTs (HiPcoTM) was mixed with P*m*PV solution ($M_w = 24{,}000$, concentration 0.1 mg/mL) in tetrahydrofuran (THF), and the mixture was sonicated for 3 h in an ice-water bath. The obtained suspension (Sus-1) was subject to centrifugation (7000*g*, 6 h) to remove the non-dispersed SWNTs. The resulting supernatant solution and sediment of SWNTs were designated as Sup-1 and Sed-1, respectively (Scheme 2). Sed-1 was collected and re-dispersed in P*m*PV solution. When the sonication–centrifugation process was repeated, the second suspension, supernatant, and sediment were designated as Sus-2, Sup-2 and Sed-2, respectively. The sonication–centrifugation process was repeated several times to disperse the tubes sufficiently, thereby allowing the tubes to have an optimum interaction with the wrapping polymer chains.

As shown in Fig. 1, the supernatant obtained from SWNTs and *cis*-P*m*PV in THF afforded a clear transparent solution. In addition, the solution gave strong near-infrared emission (Fig. 2), clearly indicating that the SWNTs have been unbundled into individual tubes (since the bundled nanotubes are non-fluorescent) [19]. The identified SWNTs are summarized in Table 1. The dispersed solution from *cis*-P*m*PV and SWNTs was quite stable for at least a few weeks before nanotube precipitation occurred. Experimental results also showed that the *cis*-P*m*PV was more effective in dispersing SWNTs than its isomer *trans*-P*m*PV, since the supernatant solution of the former consistently gave stronger NIR fluorescence signals under the same conditions. The TEM images of spin-cast films confirmed that SWNTs in a non-bundled form were well dispersed in both *cis*- and *trans*-P*m*PV (Supplemental Figure S1).

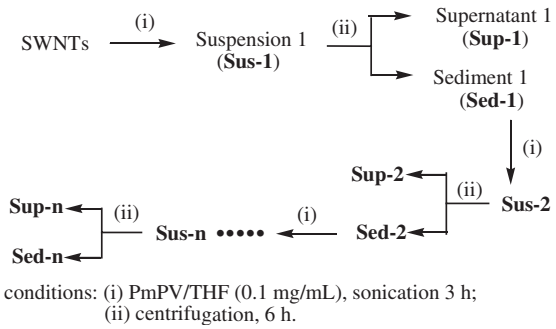

Scheme 2. The experimental procedure for wrapping of SWNTs by using *trans*-P*m*PV (**1b**) and *cis*-P*m*PV (**2b**).

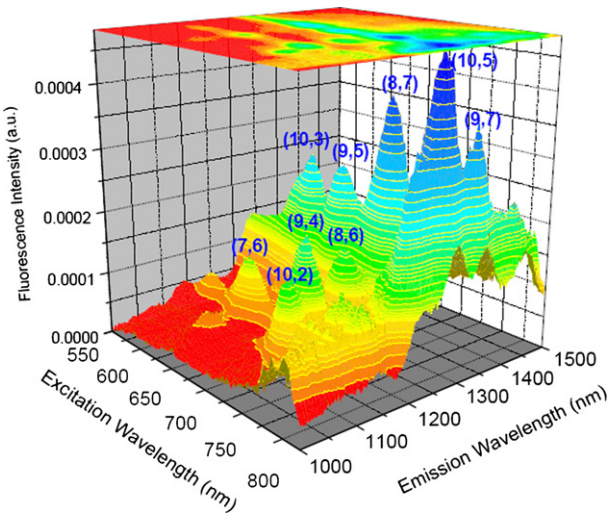

Fig. 2. 3D fluorescence spectra with a top contour plot of *cis*-P*m*PV/SWNTs solution.

Table 1
Comparison of fluorescence spectra data between *cis*-P*m*PV/SWNTs dispersion in THF and SWNTs in aqueous surfactant suspensions.

$\lambda_{ex\text{-}S}$[a] (nm)	$\lambda_{ex\text{-}R}$[b] (nm)	$\Delta\lambda_{ex}$ (nm)	$\lambda_{em\text{-}S}$[a] (nm)	$\lambda_{em\text{-}R}$[b] (nm)	$\Delta\lambda_{em}$ (nm)	Assignment	Diameter (nm)
800	786	14	1282	1250	32	(10,5)	1.050
745	728	17	1291	1267	24	(8,7)	1.032
689	671	18	1280	1244	36	(9,5)	0.976
645	633	14	1285	1250	35	(10,3)	0.936
736	716	20	1207	1172	35	(8,6)	0.966
736	720	16	1138	1101	37	(9,4)	0.916
657	647	10	1142	1122	20	(7,6)	0.895
602	587	15	1141	1113	28	(8,4)	0.840
751	734	17	1080	1053	27	(10,2)	0.794
806	790	16	1353	1323	30	(9,7)	1.103
775	756	19	1418	1380	38	(10,6)	1.111

[a] $\lambda_{ex\text{-}S}$ and $\lambda_{em\text{-}S}$ refer to excitation and emission wavelength of *cis*-P*m*PV/SWNTs dispersion samples, respectively.
[b] $\lambda_{ex\text{-}R}$ and $\lambda_{em\text{-}R}$ refers to excitation and emission wavelength of SWNTs in aqueous surfactant suspensions cited from Refs. [27,28].

2.1. Polymer conformation

Scheme 1 shows the probable structure **3** of *cis*-P*m*PV in THF solution, in which the ratio of *cis*- to *trans*-CH=CH is 2:1. The identical fluorescence λ_{max} [16,20] observed from both *cis*- and *trans*-P*m*PV indicates the presence of the structural unit **I** as the effective emission chromophore. The adjacent phenyl rings linked on a *cis*-CH=CH in the structures **II** and **III** are twisted away from *co*-planarity (by ~30°) to minimize steric interaction (Supplemental info Figure S2). Molecular modeling based on MM+ force fields, by using HyperChem (version 8.0), further shows that the chain segments are packed in relatively tight form (Fig. 3a), as a result of the *cis*-vinylene bond geometry. When an SWNT approaches the molecule, the polymer conformation partially opens up to embrace the SWNT (Fig. 3b). Simulated annealing in association with molecular dynamics can further stimulate the polymer conformation to reach the fully wrapped state (Fig. 3c), which has a lower energy as expected from a stronger π–π interaction. Examination of the polymer backbone in the fully wrapped state, however, reveals that majority of vinylene bonds are in the *trans*-configuration. It appears that the intrinsic cavity provided from *cis*-P*m*PV is too small to fit a SWNT (see Fig. 3a). Some of *cis*-vinylene bonds in **2b** have to be isomerized to *trans*-configuration in order to provide necessary cavity size to wrap around the SWNT (Scheme 3, conformation **4**).

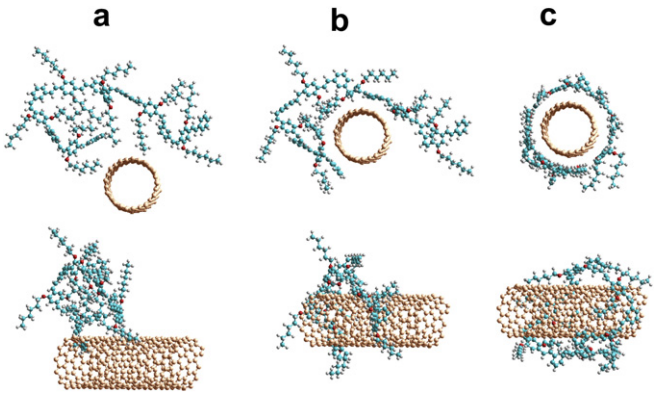

Fig. 3. Molecular modeling of *cis*-P*m*PV with (8, 7) SWNT in non-wrapped (a), partially wrapped (b), and fully wrapped states (c). The first and second rows correspond to front and side views, respectively. The three configurations have interaction energy of 61, 158, and 218 kcal/mol, respectively.

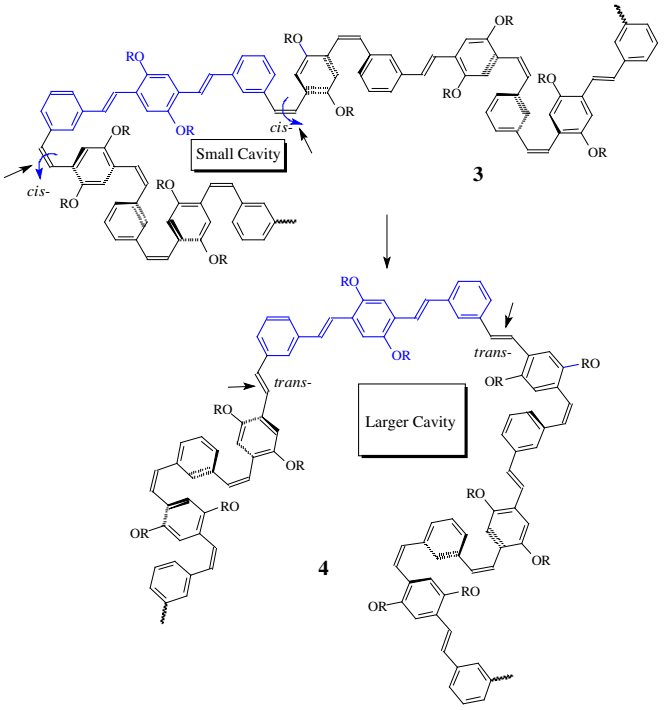

Scheme 3. Isomerization from *cis*- to *trans*-vinylene bonds (indicated by arrows) to generate a larger conformational cavity.

2.2. Absorption spectra

The individual peaks in the visible–near-infrared (Vis–NIR) spectrum can be attributed to the valence-to-conduction electronic transitions of nanotubes, which depend on the chirality of the SWNT species present in the sample solutions [21]. The absorption peak intensity is thus related to the population of the corresponding SWNT species. After interaction with the SWNTs, sonication and centrifugation, the absorption spectra were taken directly from the polymer solution of 0.1 mg/mL concentration in THF. Under the same conditions, the absorption bands of nanotubes from *cis*-P*m*PV/SWNTs suspension were about twice as high as that from *trans*-P*m*PV/SWNTs (Fig. 4). The result showed that the *cis*-P*m*PV was superior in dispersing the SWNTs than the *trans*-P*m*PV, assuming that the molar extinction coefficient of SWNTs is not affected by the wrapping polymers. Same trend was also observed in the supernatant solutions (see Supplemental info Figure S3).

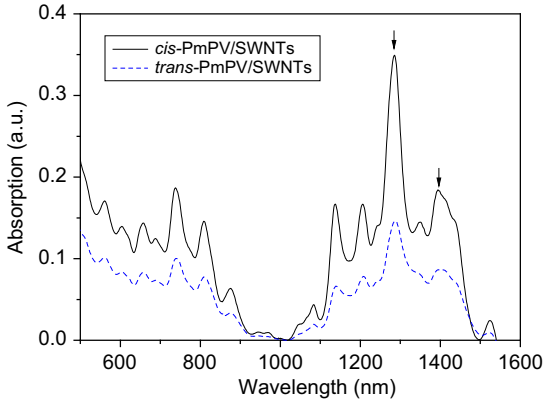

Fig. 4. UV–vis-NIR absorption spectra of *cis*-P*m*PV/SWNTs (solid line) and *trans*-P*m*PV/SWNTs (broken line) in suspension (Sus-1).

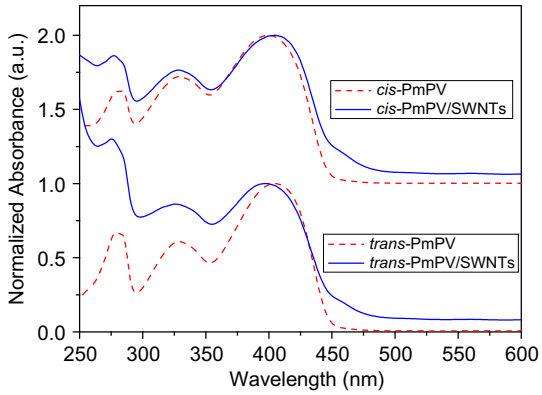

Fig. 5. UV–vis absorption spectra of *cis*- and *trans*-P*m*PV in the presence (solid line) and absence (broken line) of SWNTs. The spectra of P*m*PV/SWNTs were taken from their supernatant solution in THF.

Wrapping of SWNTs resulted in polymer chain movement, which was visible in their absorption spectra (Fig. 5). In THF solution, the absorption peak of *cis*-P*m*PV (λ_{max} = 399 nm) occurred at a shorter wavelength than that of *trans*-P*m*PV (λ_{max} = 403 nm), since the *cis*-CH=CH bond in the former prevents co-planarity (Scheme 1). Upon interaction with SWNTs, the absorption band of *cis*-P*m*PV was red-shifted by ~6 nm, while that of *trans*-P*m*PV was blue-shifted by ~7 nm. In other words, the absorption of *cis*-P*m*PV/SWNTs (λ_{max} = 405 nm) is different from that of *trans*-P*m*PV/SWNTs (λ_{max} = 396 nm), which suggests that the *cis*-P*m*PV is not simply converted to *trans*-P*m*PV via the carbon–carbon double bond isomerization. The opposite absorption pattern can be rationalized by considering the molecular conformation adjustment during the SWNTs wrapping/interaction process. For *trans*-P*m*PV, wrapping of SWNTs requires the twisting of the 2,5-dialkoxybenzene ring in order to make room to accommodate the nanotubes (Fig. 6). This chain twisting results in the blue-shifted λ_{max}. In the case of *cis*-P*m*PV, the conjugated fragment is less co-planar due to the presence of *cis*-vinylene bond. The observed spectral red-shift is attributed, at least in part, to the isomerization of *cis*-CH=CH to the corresponding *trans*-CH=CH.

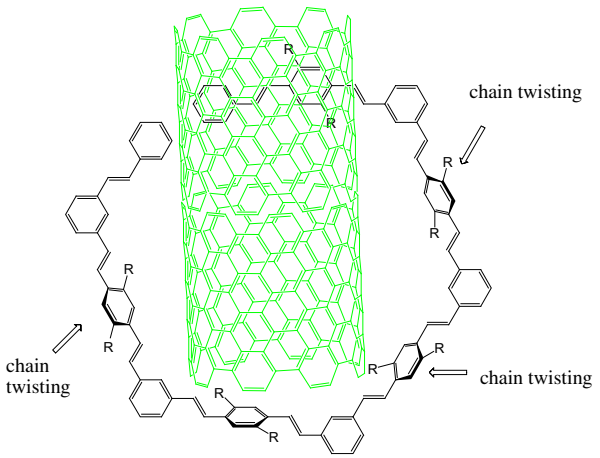

Fig. 6. Schematic illustration of *trans*-P*m*PV embracing the SWNT. The dialkoxybenzene ring is twisted away from *co*-planarity to accommodate the SWNT complexation.

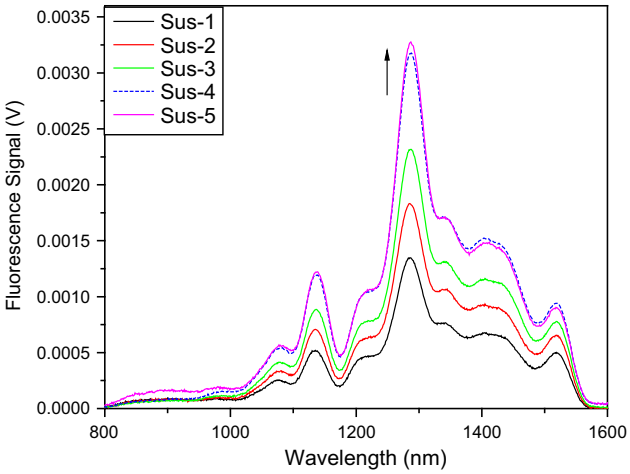

Fig. 7. Emission spectra of *cis*-P*m*PV/SWNTs in suspension series Sus-*n*.

2.3. Fluorescence

The fluorescence intensity of suspension solution was monitored to further confirm the effectiveness of SWNT dispersion, because only the single SWNT gives the emission signal. The emission intensity of the suspension quickly increased with repeated cycles of the sonication–centrifugation process (Fig. 7), as the bundled SWNTs were broken into single or individual one. The emission signal reached a maximum at about 4 cycles when using *cis*-P*m*PV, in contrast to ~7 cycles when using *trans*-P*m*PV. This result showed that the *cis*-P*m*PV was about twice as effective in dispersing SWNTs.

2.4. Raman spectra

On the basis of the previous studies [22,23,24,25], the Raman peaks at 192 cm^{-1} and 217 cm^{-1} were attributed to two metallic tubes (12, 6) and (8, 8), while the remaining peaks at 249, 257, 280, and 295 cm^{-1} to the semi-conducting (10, 3), (7, 6), (7, 5), and (8, 3) tubes, respectively (Fig. 8). For quantitative comparison, the Raman spectra were normalized against the solvent peak for comparison,

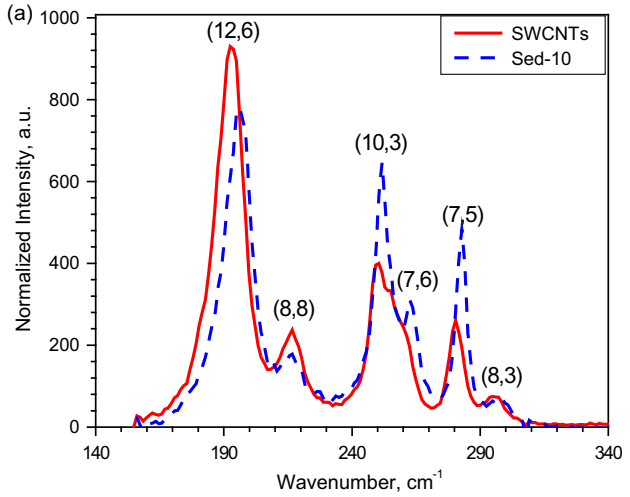

Fig. 8. Raman spectra of purified SWNTs and Sed-10 for *trans*-P*m*PV in Radial Breathing Mode (RBM). The comparison shows that the metallic tube (12, 6) is enriched in the supernatant, while semi-conducting one is enriched in the sediment.

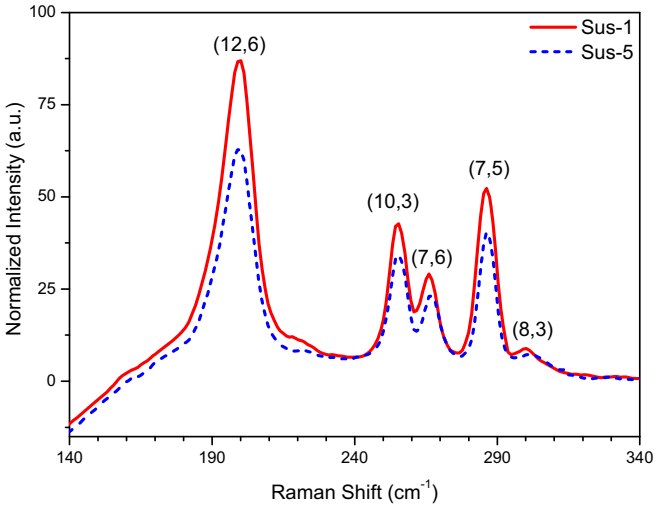

Fig. 9. Raman spectra of Sus-*n* for *cis*-P*m*PV/SWNTs in Radial Breathing Mode (RBM). The comparison shows that both the metallic or semi-conducting tubes are decreased.

since the concentration of P*m*PV solution remained to be constant throughout the study. The population of metallic (12, 6) nanotube decreased significantly (by 24.1%) from Sus-1 to Sus-7, when the *trans*-P*m*PV was used. As illustrated in Scheme 2, the nanotubes present in the suspension sample Sus-*n* should be equal to that in the preceding sediment sample Sed-($n-1$), since all the tubes in the sediment were well dispersed into the suspension. In other words, the observed enrichment of semi-conducting tubes in the suspension was equivalent to the enrichment in the sediment, which agreed well with the study of powder samples. The results from the suspension study of *trans*-P*m*PV/SWNTs, therefore, concluded that metallic tubes were enriched in the supernatant, while semi-conducting ones were enriched in the sediment.

The Raman spectra in suspension samples (Sus-*n*) also revealed the SWNT population changes (Fig. 9), although relative weaker Raman signal was detected due to the measurement in dilute solution. The Raman intensity for every single SWNT in Sus-5 was slightly lower than that in Sus-1, reflecting lower SWNT concentration in the Sus-5 sample. Analysis of the Raman data from a series of suspension samples (Sus-*n*) further showed that the population of the SWNTs was nearly unchanged in each consecutive suspension Sus-*n* (Fig. 10a) when *cis*-P*m*PV was used. This was in contrast to the suspension Sus-*n* by using *trans*-P*m*PV, where the population of the metallic SWNTs was decreasing in each consecutive suspension Sus-*n* (Fig. 10b). The nonselective dispersion from *cis*-P*m*PV could be associated with the polymer's relative poor ability to form helical conformation, in comparison with its isomeric *trans*-P*m*PV. The nonselective dispersion could also be partially attributed to *cis*-P*m*PV's higher dispersion efficiency, as the faster dispersion rate would lower the selectivity.

2.5. *cis*-/*trans*-Vinylene isomerization

The model study suggests that some of the *cis*-CH=CH bonds need to be converted to *trans*-CH=CH, in order to create necessary conformational cavity to wrap SWNTs. The ^{1}H NMR of suspension sample (sus-6) provided evidence for the isomerization of the *cis*-CH=CH to *trans*-CH=CH linkage. Without interaction with SWNTs, the resonance signals of $-OCH_2-$ in P*m*PV typically occur at about 4.1 and 3.5 ppm, which are attributed to signals from the *trans*- and *cis*-P*m*PV polymer segments, respectively [16]. Upon interaction with SWNTs, the $-OCH_2-$ signals in *trans*-P*m*PV **1b** (at ~4.1 ppm) were split into two broad signals at ~4.2 and 3.64 ppm (in about 1:1 ratio), resulting from the polymer chain's interaction with SWNTs (Fig. 11b). Similar pattern has been observed from *trans*-P*m*PV **1a** by Stoddart and co-workers [8]. In the complex of *cis*-P*m*PV **2b** with SWNTs, the $-OCH_2-$ appeared at ~4.1, 3.64, and 3.27 ppm (Fig. 11d). The signals at 4.1 and 3.64 were associated to *trans*-CH=CH segment, while that at 3.27 ppm to *cis*-CH=CH segment. The content of the *cis*-CH=CH in **2b**/SWNTs was estimated to be about 30%. It should be noted that the resonance signals near 6.3–7.0 ppm, which is also characteristic for *cis*-P*m*PV [16], were rather weak in comparison with the rest of the vinyl and phenyl protons between 7 and 8 ppm. The result further support the assumption that a notable amount of *cis*-CH=CH was transformed to *trans*-CH=CH. When heating the sample to 50 °C under vacuum for 8 h to remove the solvent residue, the *cis*-CH=CH content at 3.27 ppm was further decreased (Fig. 11e), while the two signals in *trans*-CH=CH segments at 4.1 and 3.64 ppm remained at about 1:1 ratio. The result confirmed that the $-OCH_2-$ signal at ~3.64 ppm was solely attributed to *trans*-CH=CH segment in the SWNT complex.

Isomerization from *cis*-CH=CH to *trans*-CH=CH requires to overcome a significant energy barrier (~45 kcal/mol) [26]. Typical condition for *cis*-/*trans*-isomerization in P*m*PV requires heating at 120 °C for overnight in the presence of iodine catalyst [16]. Surface contact with SWNTs appeared to facilitate the *cis*- to *trans*-isomerization, since the process occurred at a lower temperature (at ~50 °C, Fig. 11e) in the absence of catalyst. The polymer/SWNT

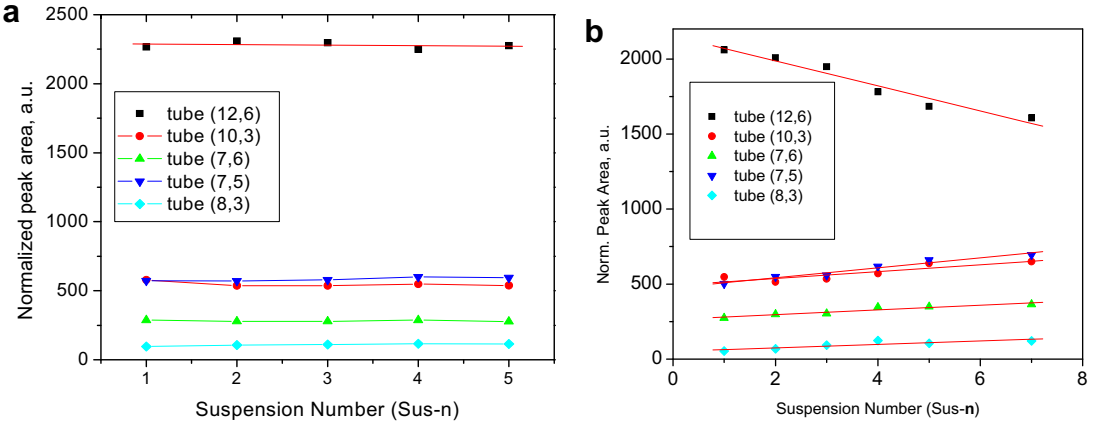

Fig. 10. The SWNT population change in consecutive suspension samples of *cis*-P*m*PV/SWNTs (a) and *trans*-P*m*PV/SWNTs (b). The plot is constructed by using the normalized RBM Raman peak area corresponding to SWNT (12, 6), (10, 3), (7, 6), (7, 5), and (8, 3).

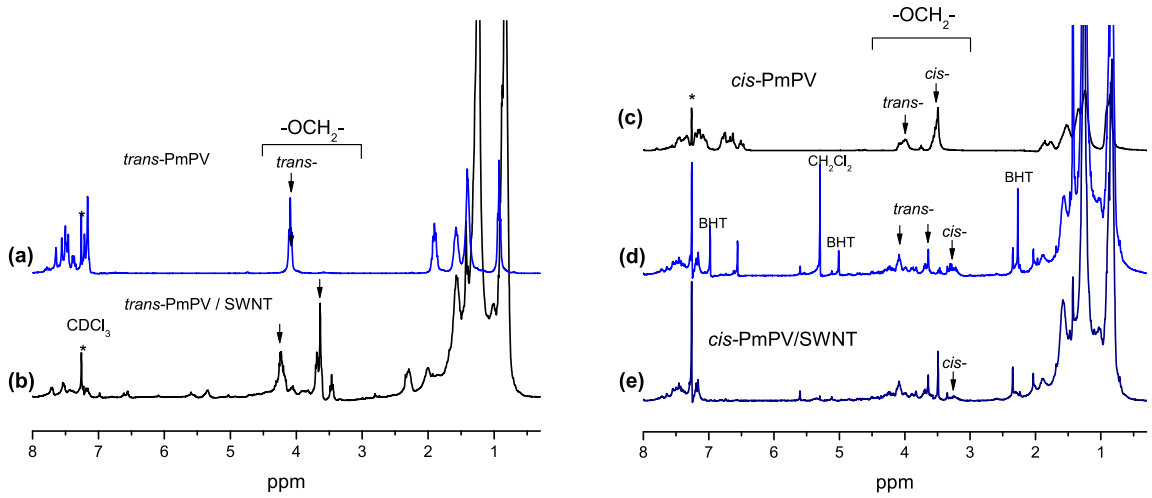

Fig. 11. Left panel: ^{1}H NMR spectrum of the *trans*-P*m*PV(**1b**)(a) and **1b**/SWNT (b) in sus-6 sample recorded in $CDCl_3$ (300 MHz). Right panel: ^{1}H NMR spectrum of *cis*-P*m*PV (**2b**) (c), 2b/SWNT complex (d) in sus-6 sample recorded in $CDCl_3$ (300 MHz). The sharp signals in the spectrum d at 6.98 (Ar-H), ~5.0 (−OH) and 2.27 (–CH_3) ppm are attributed to 2,6-di-*tert*-butyl-4-methylphenol (BHT), an additive present in THF solvent. The starred signal at 7.25 ppm is from chloroform solvent residue in $CDCl_3$. In the spectrum (e), the sample of (**2b**)/SWNT had been heated to 50 °C under vacuum for 8 h.

interaction alone, however, was not sufficient to initiate the isomerization at room temperature. When the *cis*-P*m*PV solution in THF was subjected to sonication for an hour, significant amount of *cis*-CH=CH was found to be isomerized to *trans*-CH=CH in the absence of nanotubes under the identical experimental conditions (Supplemental Figure S4). The content of *cis*-CH=CH was decreased to ~30% within an hour sonication, a comparable level observed in the sus-6 sample (Fig. 11d). In other words, the *cis*-CH=CH bonds were only partially isomerized under sonication during the SWNT wrapping process. The *cis*-/*trans*-CH=CH ratio could play an essential role in the observed higher dispersion efficiency from *cis*-P*m*PV.

2.6. Photon irradiation

The supernatant solution of *cis*-P*m*PV/SWNTs was notably more stable than *trans*-P*m*PV/SWNTs at room temperature. After a few weeks, however, a tuftlike precipitation gradually appeared and settled as a whole at the bottom (Fig. 1). It was noted that irradiation with photons of 300–500 nm greatly accelerated the precipitation process. The time requirement for precipitation of *cis*-P*m*PV/SWNTs supernatant was drastically reduced to ~1 h. Spectral analysis showed that the precipitated P*m*PV/SWNTs composite had a composition similar to that of the supernatant. It is likely that the photon absorption altered the chain conformation of P*m*PV, which deviates from the ideal conformation for wrapping SWNTs. The disturbed or distorted conformation might lead to partially unwrapping at the chain ends, which can then interact with adjacent SWNTs to form entangled species.

When a 40 W incandescent lamp was positioned in close distance (~15 cm), the entire SWNT mass floated up when the lamp was turned on (in ~10 s), and settled down when the lamp was off. This phenomenon became slower (in ~20 min) when a portable UV-lamp (365 nm) was used as the irradiation source. The fact that the entire mass was holding together during the entire process indicated that the polymer and nanotubes entangled with each other during the precipitation. This result also suggests that at least some polymer chains achieved a fully wrapped state as shown in the modeling (Fig. 3c), thereby holding the nanotubes together. While keeping the nanotubes from bundling, each polymer chain is wrapped on more than one tube and each SWNT is interacting with multiple polymer chains.

3. Conclusion

A comprehensive study showed that the poly[(*m*-phenylenevinylene)-*alt*-(*p*-phenylenevinylene)] (P*m*PV) with *cis*-vinylene bonds was a superior material for dispersing SWNTs. The unique chain conformation, which associated with the *cis*-CH=CH bond geometry, formed a suitable void among chain segments to embrace the tube. Interaction of a planar conjugated polymer fragment with the SWNT surface was demonstrated to be the primary mechanism, in consistence with the evidence from the absorption and fluorescence excitation spectra.

On the basis of absorption (Fig. 4) and fluorescence (Fig. 7), the *cis*-P*m*PV is found to be twice effective as a dispersion reagent for SWNTs than its isomeric *trans*-P*m*PV. Good solubility of *cis*-P*m*PV makes a positive contribution in dispersion, since the polymer-wrapped SWNT species would be easier to dissolve. In addition, the *cis*-P*m*PV displays similar effectiveness in dispersing all SWNTs in the sample, in contrast to its isomer *trans*-P*m*PV which shows notable selectivity toward wrapping the metallic species. The significant difference in dispersion rate and SWNT selectivity illustrates the great impact of vinylene bond geometry, which has immediate influence on the polymer conformation and its interaction with different SWNT species.

Partial isomerization of the *cis*-vinylene bond, occurred under the sonication conditions, plays an essential role to create the conformational cavity for SWNT wrapping. The observed faster dispersion rate by using *cis*-P*m*PV, than that by using *trans*-P*m*PV, is believed to attributed to the combination of polymer's good solubility and its ability to partial isomerization to *trans*-CH=CH. Incomplete isomerization suggests that the SWNT wrapping and isomerization occurs simultaneously, since the *cis*-CH=CH bonds on the wrapped polymer chain will be more difficult to isomerize to *trans*-CH=CH. The dispersion mechanism awaits to be further explored to understand the peculiar dispersion behavior.

4. Experimental

4.1. General analytical methods

Optical absorption spectra were recorded with a PerkinElmer Lambda 950 spectrophotometer at room temperature. Fluorescence spectra were measured with a Horiba-Jobin Yvon Nanolog

fluorometer, equipped with double-grating monochromator in excitation and emission, and a liquid-N_2-cooled solid state InGaAs detector (model 1427B). Measurements of Raman scattering signal were performed, either in solid (initial SWNT and Sed-10 Powder) or liquid form (Suspension series), by using the excitation wavelength of 647.1 nm from a Krypton Lexel 95 Laser. These measurements were done in the backscattering geometry, using a Horiba-Jobin Yvon Labram HR800 monochromator equipped with a nitrogen-cooled CCD camera. The elastic line was suppressed by a 647.1 nm notch filter. ^{1}H NMR spectra were collected on a Varian 300 Gemini spectrometer

4.2. Sample dispersion

The sample of SWNTs (HiPcoTM) was purified by using the procedure described previously [12]. The purified SWNTs had a low iron content (<0.05% wt%). In a typical dispersion procedure, 0.3 mg of pure SWNTs (HiPcoTM) was added to 20 mL P*m*PV solution (M_w = 24,000, concentration 0.1 mg/mL) in tetrahydrofuran (THF), and the mixture was placed in a glass vial. A sonicator probe tip was immersed in the solution mixture from the top, and the mixture was sonicated for 3 h in an ice-water bath by using a Branson Digital Sonifier (model 450). The sonication experimental condition is under18% power with 1 s *on* and 2 s *off* sequence

In the control experiment, the P*m*PV solution (0.1 mg/mL) in tetrahydrofuran (THF) was subjected to sonication (sonication condition: 15% power with 0.5 s *on* and 1 s *off* sequence for an hour in THF solvent). After removing THF solvent on a rotatory evaporator, the sample was dried under vacuum at room temperature.

Acknowledgement

YP acknowledges the financial supports from The University of Akron and NASA (Grant NNC3-1044). APS acknowledges the financial support from the Air Force through the Cooperative Center in Polymer Photonics. ML and MAM acknowledge support from NASA's Fundamental Aeronautics Program. XQW acknowledges support from NSF (DMR-0934142). We also wish to thank The National Science Foundation (CHE-9977144) for funds used to purchase the NMR instrument used in this work.

Appendix. Supplementary data

Supplementary data associated with this article can be found in the online version, at doi:10.1016/j.polymer.2009.11.052.

References

[1] Meyyappan M. Carbon nanotubes: science and applications. New York: CRC Press; 2005.
[2] Ahn J-H, Kim H-S, Lee KJ, Jeon S, Kang SJ, Sun Y, et al. Science 2006;314:1754–7.
[3] Kauffman DR, Star A. Chem Soc Rev 2008;37:1197–206.
[4] Lemieux MC, Roberts M, Barman S, Jin YW, Kim JM, Bao Z. Science 2008;321:101–3.
[5] Tasis D, Tagmatarchis N, Bianco A, Prato M. Chem Rev 2006;106:1105–36.
[6] Panhuis MIH, Maiti A, Dalton AB, van den Noort A, Coleman JN, McCarthy B, et al. J Phys Chem B 2003;107:478–82.
[7] Coleman JN, Dalton AB, Curran S, Rubio A, Davey AP, Drury A, et al. Adv Mater 2000;12:213–6.
[8] Star A, Stoddart JF, Steuerman D, Diehl M, Boukai A, Wong EW, et al. Angew Chem Int Ed Engl 2001;40:1721–5.
[9] Star A, Liu Y, Grant K, Ridvan L, Stoddart JF, Steuerman DW, et al. Macromolecules 2003;36:553–60.
[10] Dalton AB, Stephan C, Coleman JN, McCarthy B, Ajayan PM, Lefrant S, et al. J Phys Chem B 2000;104:10012–6.
[11] Keogh SM, Hedderman TG, Lynch P, Farrell GF, Byrne HJ. J Phys Chem B 2006;110:19369–74.
[12] Yi W, Malkovskiy A, Chu Q, Sokolov AP, Colon ML, Meador M, et al. J Phys Chem B 2008;112:12263–9.
[13] Curran SA, Ajayan PM, Blau WJ, Carroll DL, Coleman JN, Dalton AB, et al. Adv Mater 1998;10:1091–3.
[14] Woo HS, Czerw R, Webster S, Carroll DL, Ballato J, Strevens AE, et al. Appl Phys Lett 2000;77:1393–5.
[15] Star A, Lu Y, Bradley K, Gruner G. Nano Lett 2004;4:1587–91.
[16] Pang Y, Li J, Hu B, Karasz FE. Macromolecules 1999;32:3946–50.
[17] Keogh SM, Hedderman TG, Gregan E, Farrell G, Chambers G, Byrne HJ. J Phys Chem B 2004;108:6233–41.
[18] Dalton AB, Coleman JN, Panhuis M, McCarthy B, Druby A, Blau WJ, et al. J Photochem Photobiol A 2000;144:31–4.
[19] O'Connell MJ, Bachilo SM, Huffman CB, Moore VC, Stano MS, Haroz EH, et al. Science 2002;297:593–6.
[20] Liao L, Pang Y, Ding L, Karasz FE. J Polym Sci Part A Polym Chem 2004;42:1820–9.
[21] Tu X, Manohar S, Jagota A, Zheng M. Nature 2009;460:250–3.
[22] Jorio A, Saito R, Hafner JH, Lieber CM, Hunter M, McClure T, et al. Phys Rev Lett 2001;86:1118–21.
[23] Telg H, Maultzsch J, Reich S, Hennrich F, Thomasen C. Phys Rev Lett 2004;93:177401.
[24] Fantini C, Jorio A, Souza M, Strano MS, Dresselhaus MS, Pimenta MA. Phys Rev Lett 2004;93:147406.
[25] Hennrich F, Krupke R, Lebedkin S, Arnold K, Fischer R, Resasco DE, et al. J Phys Chem B 2005;109:10567–73.
[26] Meier H. Angew Chem Int Ed 1992;31:1399–540.
[27] Bachilo SM, Strano MS, Kittrell C, Hauge RH, Smalley RE, Weisman B. Science 2002;298:2362–6.
[28] Weisman RB, Bachilo SM. Nano Lett 2003;3:1235–8.